A NOVEL TRIPLE PASSBAND FILTER DESIGN METHOD BASED ON STEPPED IMPEDANCE RESONATORS

Z.-P. Li[*], S. J. Wang, T. Su, and C. H. Liang

Key Laboratory of Science and Technology on Antennas and Microwaves, Xidian University, Xi'an, Shaanxi 710071, People's Republic of China

Abstract—In this letter, a novel compact tri-band bandpass filter (BPF) with high selectivity is presented. The proposed tri-band performance measure is realized by using eight sets of resonators, i.e., two- and three-section stepped impedance resonators (SIRs). The three-section SIR is designed for determining the three passbands and providing the electric coupling, while the two-section SIR is used for determining each passband respectively and providing the magnetic coupling. Then, coupling structures with two transmission zeros near each passband edge are presented, therefore, the band selectivity of the filter is much improved. The three passband frequencies could be independently designed and tuned. This novel tri-band BPF is fabricated and the measured results are in good agreement with the full-wave simulation results.

1. INTRODUCTION

RF/microwave filters play a very important and essential role in modern wireless and mobile communication systems. Planar filters using printed circuit technology are becoming particularly popular owing to their low-cost, compact size and light weight [1]. Therefore, many techniques applied to planar filter design such as parallel- and cross-coupling have been widely used in microwave communication systems owing to its advantage of ease in manufacture, simplicity in synthesis.

In recent years, multiservice wireless systems have been gaining much more attention. Multi-band filters become quite popular.

Therefore, they had been widely studied in several papers [2–13]. In [2], a tri-band filter was designed using three sets of resonators with a common feed circuit, but it has a large size due to a large number of resonators. In [3], based on a dual-plane microstrip/DGS slot structure, a tri-band filter with improved band allocation was proposed. In [4], the design of a tri-band filter uses parallel coupled structure between two stub-loaded resonators to obtain extra transmission zeros near three passbands edges. A tri-band filter was designed using only one set of resonators presented in [5]. Resonators with controllable second and third harmonics and stub-loaded resonators have been used to generate three passbands. And some other design procedures about multi-band filter have been discussed in paper [7–13].

In this letter, a fourth-order tri-band chebyshev BPF is designed using two- and three-section stepped impedance resonators on a single-layer substrate. The frequency characteristics of SIRs are presented in Section 2. By properly determining the impedance ratios and physical lengths of SIRs, three passbands can be obtained. Besides that, the BPF consists of three cascaded quadruplets (CQs) with two transmission zeros near each passband edge. Another three extra transmission zeros can be obtained by using the skew-symmetrical ($0°$) feeding structure. Rigorous design procedure is introduced in Section 3. The measured results exhibit a tri-band feature of three passbands at 2.5, 3.8 and 5.9 GHz, which are in good agreement with the full-wave results.

2. DETERMINE THE RESONANCE BEHAVIORS OF TWO- AND THREE-SECTION SIRS

The two-section SIR has been introduced in many papers[11, 14, 18]. As shown in Fig. 1, when $\theta_1 = \theta_2 = \theta_0$, ratios of the higher-order resonant frequencies to the fundamental frequency (f_{s1}/f_0 and f_{s2}/f_0)
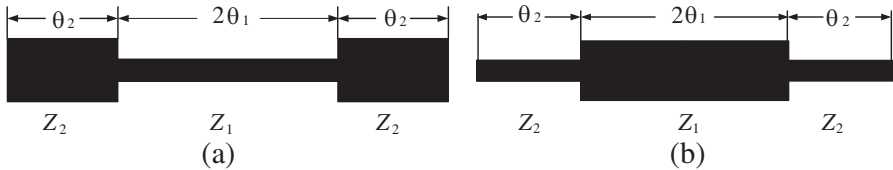

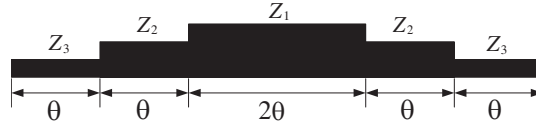**Figure 1.** Half-wave SIR: (a) $K < 1$, (b) $K > 1$.

Figure 2. Half-wave three section SIR.

for half-wavelength SIR are characterized by

$$\frac{f_{s1}}{f_0} = \frac{\theta_{s1}}{\theta_0} = \frac{\pi}{2\arctan\sqrt{K}} \tag{1a}$$

$$\frac{f_{s2}}{f_0} = \frac{\theta_{s2}}{\theta_0} = \frac{\pi}{\arctan\sqrt{K}} - 1 \tag{1b}$$

where K is the impedance ratio, $K = Z_2/Z_1$.

Note that, from formula 1, the three variables (f_0, f_{s1} and f_{s2}) are not independent completely. In other words, when both f_0 and f_{s1} are fixed, f_{s2} is also determined. So, the two-section SIR cannot satisfy to determine the three passbands independently.

In order to obtain any of frequency responses, the three-section SIR should be introduced. As shown in Fig. 2, the input admittance can be shown

$$Y_i = j\frac{1}{z_3}\frac{2(1+k_1+k_2+k_1k_2)\big[k_1k_2-(1+k_1+k_2)\tan^2\theta\big]\tan\theta}{k_1k_2(1+k_1+k_2)(1-\tan^2\theta)^2-2\big[(1+k_1+k_2)^2+k_1^2k_2^2\big]\tan^2\theta} \tag{2}$$

where k_1 and k_2 are the impedance ratios, $k_1 = Z_3/Z_2$ and $k_2 = Z_2/Z_1$. The fundamental frequency of three-section SIR is shown as follows:

$$\theta = \arctan\sqrt{\frac{k_1k_2}{k_1+k_2+1}} \tag{3}$$

For three-section SIR, ratios of the higher-order resonant frequencies to the fundamental frequency (f_{s1}/f_0 and f_{s2}/f_0) can be derived as

$$\frac{f_{s1}}{f_0} = \frac{\theta_{s1}}{\theta_0} = \frac{\arctan\sqrt{\frac{1+k_1+k_1k_2}{k_2}}}{\arctan\sqrt{\frac{k_1k_2}{1+k_1+k_2}}} \tag{4a}$$

$$\frac{f_{s2}}{f_0} = \frac{\theta_{s2}}{\theta_0} = \frac{\pi}{2\arctan\sqrt{\frac{k_1k_2}{1+k_1+k_2}}} \tag{4b}$$

By appropriately choosing combinations of k_1 and k_2, we can control the position of the fundamental frequency and higher harmonics arbitrarily to obtain the desired frequency responses.
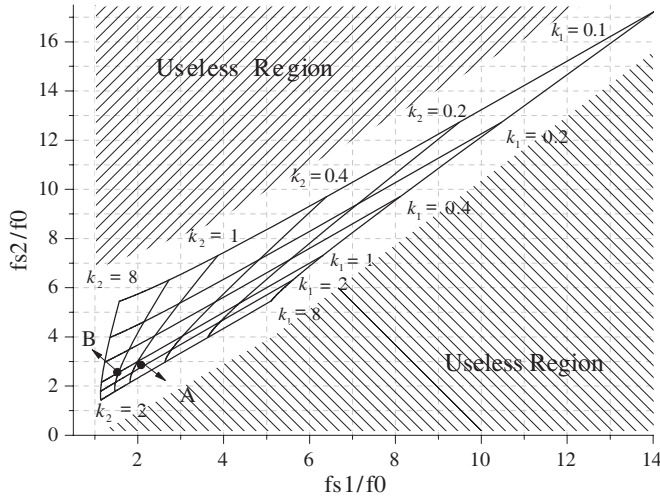
Figure 3. Design graph for three-section stepped-impedance resonators.

Figure 3 shows the normalized ratios of higher resonant frequencies to the fundamental resonant frequency for the three-section SIR with both k_1 and k_2 changing from 0.1 to 8. When both k_1 and k_2 are simultaneously equal to one (point A in Fig. 3), the three-section SIR degenerates to the traditional half-wave resonator whose harmonic is the multiples of its fundamental frequency. And also, we can obtain the designed frequencies ratios from Fig. 3. For example, if a resonator is required with $f_{s1}/f_0 = 1$ and $f_{s2}/f_0 = 2$, one can locate point B with $k_1 = 1$ and $k_2 = 2$ to satisfy the given specifications. It should be noticed that some ratios of the higher-order resonant frequencies to the fundamental frequency cannot be reached because they are in the useless region.

3. BASIC THEORY OF TRI-BAND FILTER

Figure 4(a) describes a coupled structure for tri-band filters. Both $R1$ and $R4$ resonators can work at three resonance frequencies f_1, f_2 and f_3 simultaneously, while the other six resonators with superscripts, $R2^{I}$ and $R3^{I}$, $R2^{II}$ and $R3^{II}$, $R2^{III}$ and $R3^{III}$, can only resonate at one of the three resonance frequencies. Then, three passbands can be designed independently. In other words, each of the coupling coefficients between adjacent resonators can be extracted separately at the three specific passbands. In order to improve the selectivity of
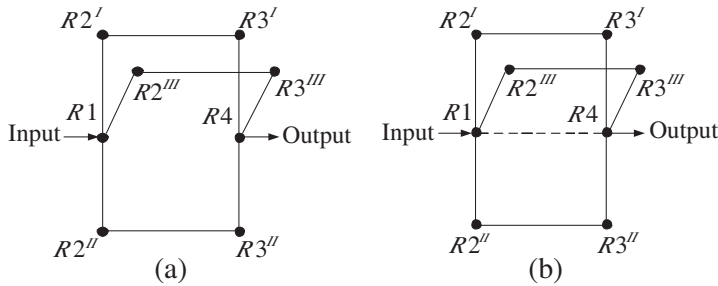
Figure 4. Coupling structures of: (a) Direct-coupled tri-band filter with fourth-order response. (b) Cross-coupled filters with fourth-order response.

the filterthe coupling structures of dual- and triple-band filters with a general chebyshev frequency response have also been proposed. As shown in Fig. 4(b), the solid lines represent direct coupling, while the dotted ones represent crossing coupling. Thus a pair of transmission zeros can be introduced in low and high part of each passband, and a much sharper filter skirt and higher selectivity can be achieved.

4. DESIGN OF A TRI-BAND BANDPASS FILTER

In this design example, a general chebyshev filter with a triple-passband response is realized with compact folded two- and three-section SIR as the building block. Its coupling structure is based on the structure shown in Fig. 4(b). The first step is to determine the impedances of SIRs. In order to guarantee to resonate simultaneously at the center frequencies of the three passbands, 2.5 GHz, 3.8 GHz and 5.9 GHz, the realizable impedances of three-section SIR should be $Z_1 = 50$ and $Z_2 = 70$, $Z_3 = 140$ and $\theta = 0.21\pi$. With two-section SIRs, their fundamental frequencies should locate at the designed positions and the harmonics must be placed outside the three passbands to avoid an impact on the design of the passbands. Table 1 summarizes the impedances.

The second step is to determine the external quality factor. The Fig. 5(a) shows the configuration of a tapped three-section SIR.
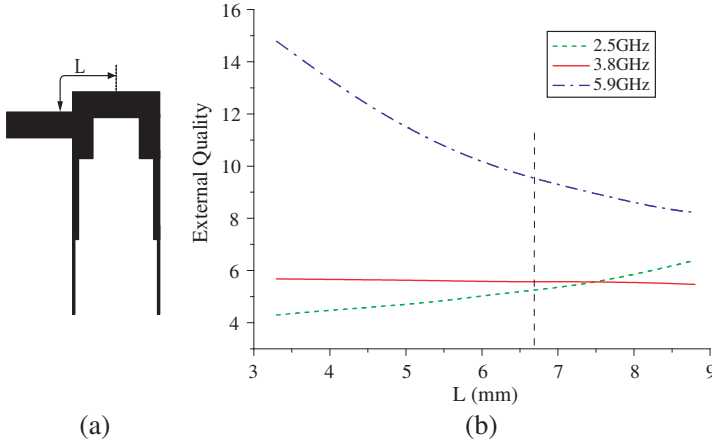
By neglecting transmission line losses, the loaded quality factor Q_e is given as:

$$Q_e = R_0 \frac{\omega_0}{2} \frac{dB}{d\omega} |_{\omega=\omega_0} \tag{5}$$

where R_0 is the characteristic impedance, ω_0 the angular operating

Table 1. Impedances of two-section SIRs.

fundamental frequency (GHz)	Impedances (ohm)	
	Z_1	Z_2
2.5	123.5	50
3.8	82.7	70
5.9	98.4	80

(a)   (b)

Figure 5. (a) The circuit model for calculating Q_e. (b) External qualities at 2.5, 3.8 and 5.9 GHz.

frequency, and B the total susceptance of the resonator seen from the feedline at the tapping point.

For this specific circuit, B can be written as:

$$Y_{in} = Y_0 \frac{Y_r + jY_0 \tan \theta_0}{Y_0 + jY_r \tan \theta_0} \tag{6}$$

with

$$Y_r = Y_1 \frac{2Y_1 Y_a + j\left(Y_1^2 + Y_a^2\right)\left(\tan \theta_m + \tan \theta_n\right) - 2Y_1 Y_a \tan \theta_m \tan \theta_n}{(Y_1 + jY_a \tan \theta_m)(Y_1 + jY_a \tan \theta_n)} \tag{7}$$

where

$$Y_a = Y_2 \frac{(Y_1 + Y_2) \tan \theta}{Y_2 + Y_1 \tan^2 \theta} \quad \text{and} \quad \theta_m + \theta_n = 2\theta \tag{8}$$

Figure 5(b) illustrates the external quality factor calculated by formula (5) to (8). With L varies from 3.5 to 8.5 mm, the external

quality factor of the first increases gradually, while the second almost keeps constant and the third reduces gradually. Thus, with different distance L, the combination of bandwidth is different. Here we choose the three external qualiy factors at the intersections of the solid lines and the dash line in Fig. 5(b). Because the filter order and the ripple level are specified and identical at the three passbands, the ratio of the three band widths is approximately $1 : 1.1 : 1.8$. For this specific circuit, the 3 dB fractional bandwidths (FBW) of these three passbands are set as 3.5%, 3.8%, and 4.5% responding to the 2.5, 3.8, and 5.9 GHz, respectively.

$$m_{\text{normalized}} = \begin{bmatrix} 0 & 0.9137 & 0 & 0 & 0 & 0 \\ 0.9137 & 0.0027 & 0.7999 & 0 & -0.0135 & 0 \\ 0 & 0.7999 & 0.0056 & 0.6487 & 0 & 0 \\ 0 & 0 & 0.6487 & -0.0350 & 0.7995 & 0 \\ 0 & -0.0135 & 0 & 0.7995 & 0.0027 & 0.9137 \\ 0 & 0 & 0 & 0 & 0.9137 & 0 \end{bmatrix}$$

where $M_{i,j} = \frac{\text{FBW}}{f_0} m_{ij}$, $Q_{ext,s} = \frac{1}{(\text{FBW}/f_0)m_{s1}^2}$ and $Q_{ext,l} = \frac{1}{(\text{FBW}/f_0)m_{12l}^2}$. In general, $Q_{ext,s}$ is equal to $Q_{ext,l}$.

The third step is determine the coupling coefficient by [19]

$$M_{i,j} = \pm \frac{f_{p2}^2 - f_{p1}^2}{f_{p2}^2 + f_{p1}^2} \tag{9}$$

where f_{p1} and f_{p2} denote the two coupled resonant frequencies of the resonators.

Figure 6 describes the tendency of coupling coefficient varying with coupling distance. The appropriate coupling coefficient can be chosen in it. Note that the coupling coefficient M_{14} is electric coupling, M_{12}, M_{23} and M_{34} represent the magnetic coupling. The phase responses of the magnetic and mixed coupling structures are out of phase with the electric coupling structure, showing opposite signs of them.

The design procedure of passbands at 3.8 GHz and 5.9 GHz is the same as that of a passband at 2.5 GHz. It would not be discussed again. Their coupling matrices are shown below and coupling coefficients are described in Fig. 7.

For 3.8 GHz

$$m_{\text{normalized}} = \begin{bmatrix} 0 & 0.9109 & 0 & 0 & 0 & 0 \\ 0.9109 & -0.0129 & 0.7918 & 0 & -0.0578 & 0 \\ 0 & 0.7918 & -0.0371 & 0.6597 & 0 & 0 \\ 0 & 0 & 0.6597 & 0.17840 & 0.7814 & 0 \\ 0 & -0.0578 & 0 & 0.7814 & -0.0129 & 0.9109 \\ 0 & 0 & 0 & 0 & 0.9109 & 0 \end{bmatrix}$$
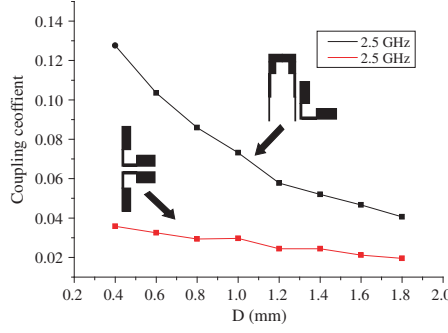
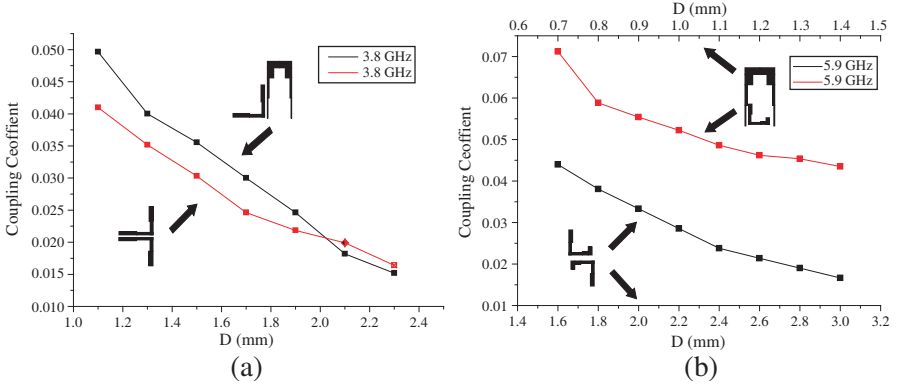**Figure 6.** Coupling coefficient at 2.5 GHz

Figure 7. (a) and (b): the coupling coefficient at 3.8 and 5.9 GHz.

For 5.9 GHz

$$m_{\text{normalized}} = \begin{bmatrix} 0 & 0.9132 & 0 & 0 & 0 & 0 \\ 0.9132 & -0.0095 & 0.7985 & 0 & -0.0216 & 0 \\ 0 & 0.7985 & -0.0208 & 0.6428 & 0 & 0 \\ 0 & 0 & 0.6428 & 0.1227 & 0.7936 & 0 \\ 0 & -0.0216 & 0 & 0.7936 & -0.095 & 0.9132 \\ 0 & 0 & 0 & 0 & 0.9132 & 0 \end{bmatrix}$$

The last step is to put all the SIRs combination. The developed filter topology is shown in Fig. 8(a). And Fig. 8(b) is the photograph of the filter. The size of this resulting circuit is about 60×60 mm, approximately $0.23\lambda_g \times 0.24\lambda_g$, where λ_g is the guided wavelength on the substrate at the center frequency of the first passband. The simulated and measured results of the filter are shown in Fig. 8(c). Two
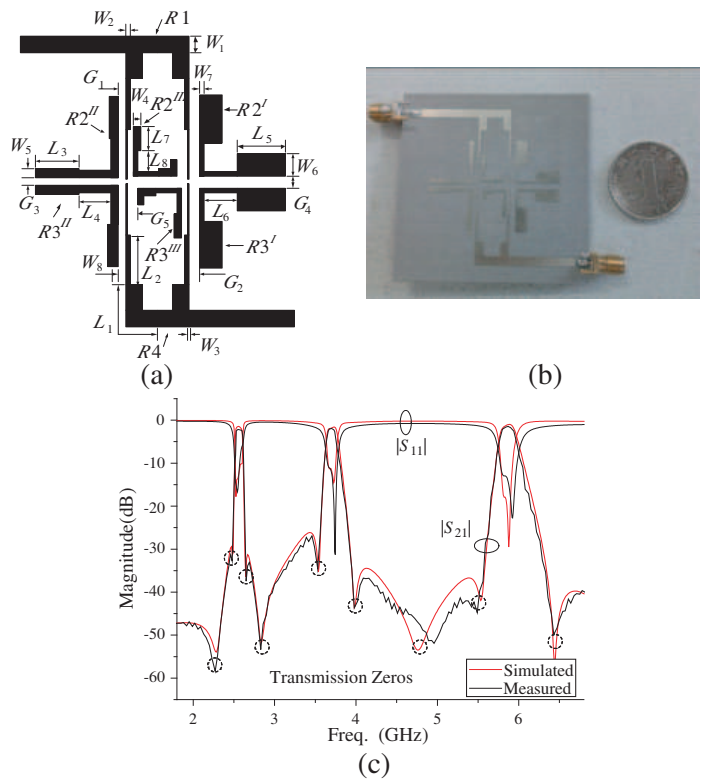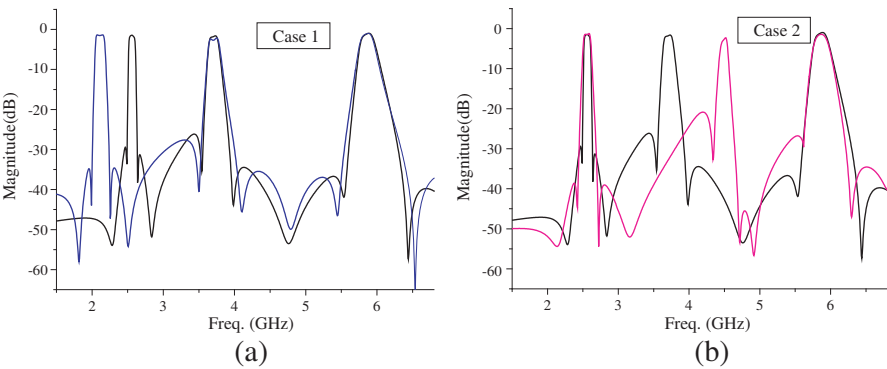
(a)   (b)

(c)

Figure 8. (a) Schematic layout, (b) photograph of fabricated microstrip filter, and (c) measured and simulated frequency response of the fabricated filter. $L_1 = 6.7$, $L_2 = 8.6$, $L_3 = 7.2$, $L_4 = 6.6$, $L_5 = 7.9$, $L_6 = 6.2$, $L_7 = 4.2$, $L_8 = 4.3$, $W_1 = 2.8$, $W_2 = 0.8$, $W_3 = 0.3$, $W_4 = 1.2$, $W_5 = 1.6$, $W_6 = 3.8$, $W_7 = 0.8$, $W_8 = 1.2$, $G_1 = 1.2$, $G_2 = 1.9$, $G_3 = 1.2$, $G_4 = 1.7$, $G_5 = 1.7$ (all in mm).
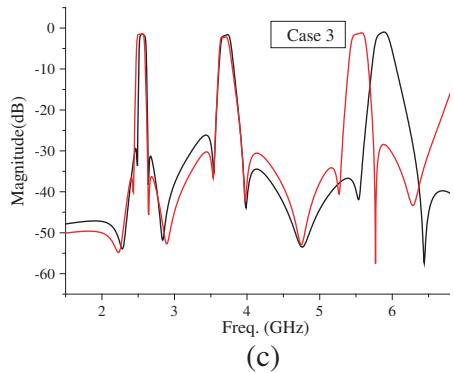

(a)   (b)

(c)

Figure 9. The Insertion loss with different impedance ratios.

Table 2. Performance comparison between the proposed tri-band filter and other techniques.

	1st/2nd/3rd Passband (GHz)	$|S_{21}|$ (dB)	$|S_{11}|$ (dB)	FBW (%)
Ref. [15]	1/2.4/3.6	2.2/1.8/1.7	20/40/35	5/2.1/1.4
Ref. [16]	1/2.4/3.6	2/1.9/1.7	15/35/20	5/2.1/1.4
Ref. [17]	2.4/4.8/7.2	1.7/0.9/0.7	15/23/18	5.3/6/8.7
Ref. [18]	2.5/3.5/5.2	2/2.4/1.7	18/16/13	2.5/1.7/5
Proposed Filter	2.5/3.8/5.9	2.1/1.9/2.3	18/30/22	3.5/3.8/4.5
	Pole Number	Independent Control	physical dimensions (mm)	
Ref. [15]	2	No	60×60	
Ref. [16]	2	No	40×40	
Ref. [17]	6	No	22×15	
Ref. [18]	5	Yes	22×30	
Proposed Filter	9	Yes	60×60	

transmission zeros near each passband edges are also observed, which is due to the cross coupling resonators. It is seen that the measured and simulated results are in good agreement. The measured fractional bandwidths are 3.5%, 3.8% and 4.5%. The measured passband return losses at all bands are below 13 dB, while the passband insertion

losses are approximately 2.1, 1.9, and 2.3 dB at 2.5, 3.8, and 5.9 GHz, respectively.

From the above design procedure, it is obvious that both the centers and the coupling coefficients of the three passbands can be devised independently, and the passbands barely interfere each other. As shown in Fig. 9, when $k_1 = 1$, $k_2 = 1.3$, only the first passband moves while the other two almost does not move (Case 1). When $k_1 = 3$, $k_2 = 3$, only the second passband moves while the first and third do not move (Case 2). And When $k_1 = 4$, $k_2 = 5$, only the third passband moves while the first and second do not move (Case 3).

Table 2 summarizes the comparison of the proposed filter with those previously reported. The triple-band general chebyshev BPF has the advantage of high selectivity, compact size and independent control of passband locations. As a result, it is quite useful for multiservice applications in future mobile communication systems.

5. CONCLUSION

In this letter, a planar tri-band BPF with compact size, high selectivity is presented, which has good tri-passband performance at 2.5, 3.8, 5.9 GHz, with the FBW 3.5%, 3.8%, and 4.5%. The passband frequencies can be conveniently tuned to desired values by controlling the ratios of SIRs, so this filter can control band locations independently. And nine transmission zeros are realized. Six of them are provided by crossing couplings, and the rest of them provided by skew-symmetrical ($0°$) feeding structure. The proposed tri-band microstrip BPF has been fabricated on a 1-mm-thick substrate with the permittivity 2.65, and the measurements are in great agreement with the simulation.

REFERENCES

1. Pozar, D. M., *Microwave Engineering*, 2nd Edition, Ch. 8, Wiley, New York, 1998.
2. Weng, M.-H. and H.-W. Wu, "A novel triple-band bandpass filter using multilayer-based substrates for WiMAX," *Proc. Eur. Microw. Conf.*, 325–328, Oct. 2007.
3. Ren, L.-Y., "Tri-band bandpass flters based on dual-plane microstrip/DGS Slot Structure," *IEEE Microw. Wirel. Compon. Lett.*, Vol. 20, No. 8, 429–431, 2010.
4. Zhang, X.-Z., Q. Xue, and B.-J. Hu, "Planar tri-band bandpass

filter with compact size," *IEEE Microw. Wirel. Compon. Lett.*, Vol. 20, No. 5, 262–264, 2010.

5. F.-C. Chen, Q.-X. Chu, and Z.-H. Tu, "Tri-band bandpass filter using stub loaded resonators," *Electron. Lett.*, Vol. 44, No. 12, 747–749, Jun. 2008.

6. Wang, X.-H., B.-Z. Wang, and K. J. Chen, "Compact broadband dual-band bandpass filters using slotted ground structures," *Progress In Electromagnetics Research*, Vol. 82, 151–166, 2008.

7. Fan, J.-W., C.-H. Liang, and X.-W. Dai, "Design of cross-coupled dual-band filter with equal-length split-ring resonators," *Progress In Electromagnetics Research*, Vol. 75, 285–293, 2007.

8. Wu, M.-S., Y.-Z. Chueh, J.-C. Yeh, and S.-G. Mao, "Synthesis of triple-band and quad-band bandpass filters using lumped-element coplanar waveguide resonators," *Progress In Electromagnetics Research B*, Vol. 13, 433–451, 2009.

9. Liu, Y., W.-B. Dou, and Y.-J. Zhao, "A tri-band bandpass filter realized using tri-mode T-shape branches," *Progress In Electromagnetics Research*, Vol. 105, 425–444, 2010.

10. Chen, W.-Y., M.-H. Weng, S.-J. Chang, H. Kuan, and Y.-H. Su, "A new tri-band bandpass filter for GSM, WiMAX and ultra-wideband responses by using asymmetric stepped impedance resonators," *Progress In Electromagnetics Research*, Vol. 124, 365–381, 2012.

11. Lin, W.-J., C.-S. Chang, J.-Y. Li, D.-B. Lin, L.-S. Chen, and M.-P. Houng, "A new approach of dual-band filters by stepped impedance simplified cascaded quadruplet resonators with slot coupling," *Progress In Electromagnetics Research Letters*, Vol. 9, 19–28, 2009.

12. Wu, G.-L., W. Mu, X.-W. Dai, and Y.-C. Jiao, "Design of novel dual-band bandpass filter with microstrip meander-loop resonator and CSRR DGS," *Progress In Electromagnetics Research*, Vol. 78, 17–24, 2008.

13. De Paco, P., O. Menendez, and J. Marin, "Dual-band filter using non-bianisotropic split-ring resonators," *Progress In Electromagnetics Research Letters*, Vol. 13, 51–58, 2010.

14. Sagawa, M., M. Makimoto, and S. Yamashita, "Geometrical structures and fundamental characteristics of microwave stepped-impedance resonators," *IEEE Trans. on Microw. Theory and Tech.*, Vol. 45, No. 7, 1078–1084, 2002.

15. Lin, X. M. and Q. X. Chu, "Design of triple-band bandpass filter using tri-section stepped-impedance resonators," *Proc. Int.*

Microw. Millimeter Wave Tech. Conf., 798–800, Guilin, China, Apr. 2007.

16. Chu, Q. X. and X. M. Lin, "Advanced triple-band bandpass filter using tri-section SIR," *Electron. Lett.*, Vol. 44, No. 4, 295–296, Feb. 2008.

17. Luo, S., L. Zhu, and S. Sun, "Compact dual-mode triple-band bandpass filters using three pairs of degenerate modes in a ring resonator," *IEEE Trans. on Microw. Theory and Tech.*, Vol. 59, No. 5, 1222–1229, May 2011.

18. Chen, F. C. and Q. X. Chu, "Design of compact tri-band bandpass filters using assembled resonators," *IEEE Microw. Theory Tech.*, Vol. 57, No. 1, 165–171, Jan. 2009.

19. Hong, J.-S. and M. J. Lancaster, *Microstrip Filters for RF/Microwave Applications*, Wiley, New York, 2001.